E-157: A PLASMA WAKEFIELD ACCELERATION EXPERIMENT

P. Muggli[*], M.J. Hogan[†], C.E. Clayton[§], S. Wang[§], R.H. Siemann[†], B.E. Blue[§], S. Lee[*],
P. Raimondi[†], R.H. Iverson[†], D. Walz[†], R. Assmann[+], K.A. Marsh[§], F.-J. Decker[†],
E.S. Dodd[§], C. Joshi[§,] T. Katsouelas[*], W.B. Mori[§]

[*]*University of Southern California, Los Angeles, CA, USA*
[†]*Stanford Linear Accelerator Center, Menlo Park, CA, USA*
[§]*University of California at Los Angeles, CA, USA*
[+]*CERN, Switzerland*

Abstract

The E-157 plasma wakefield experiment addresses issues relevant to a meter long plasma accelerator module. In particular, a 1.4 m long plasma source has been developed for the experiment. The transverse dynamics of the beam in the plasma is studied: multiple betatron oscillations of the beam envelope, flipping of the beam tail, stability against the hose instability, emission of synchrotron radiation by the beam in the plasma. The bending of the 28.5 GeV beam at the plasma/vapor interface is observed for the first time. The longitudinal dynamics of the beam, i.e. the energy loss and gain by the electrons in the wake, is strongly affected by the oscillation of the beam tail.

1 INTRODUCTION

Plasmas can sustain electric fields orders of magnitude larger than conventional rf structures. In a plasma, the frequency of the accelerating electrostatic (es) field is the plasma electron frequency ($_p=(n_p e^2/ m_e)^{1/2}$), and can reach 1-3 THz with plasma density n_p in the 10^{16} cm^{-3} range. Recently electrons (e$^-$) have been accelerated from rest to energies up to 100 MeV in waves or wakes driven by short laser pulses [1]. In the Plasma Wakefield Accelerator (PWFA) a relativistic e$^-$ bunch is sent in a neutral plasma. The space charge field of the e$^-$ bunch pushes the plasma e$^-$ and drives the plasma wake. The wake has a wavelength $_p=2 c/$, and follows the driving the e$^-$ bunch, much the same as the water wake behind a boat. Electrons located in the accelerating phase of the wake can gain energy at very high rates (100 MeV/m to multi-GeV/m).

The key experimental issues that must be addressed to demonstrate the viability of the PWFA as a high-energy particle accelerator are the following:

- The production of meter long, low atomic number plasmas with e$^-$ densities in the 10^{14}-10^{17} e$^-$/cm^{-3} range.
- The study of transverse dynamics of e$^-$ the beam, and the demonstration of the matching of the beam to the plasma.

- The demonstration of the stability of the beam propagating in the plasma against the e$^-$ hose instability.
- The understanding of the longitudinal dynamics of the particles loosing energy to the wake, and of the particles gaining energy from the wake.
- The verification of the scaling laws of the PWFA that will allow for the extension of the present experiments to multi-GeV/m accelerator modules.
- The acceleration and focusing of both electrons and positrons.

The E-157 PWFA experiment [2] performed at the Stanford Linear Accelerator Center (SLAC) is the first experiment to address these issues with a meter-long plasma accelerator module. In this paper the characteristics of the PWFA wake are first briefly reviewed. Second, the E-157 experimental apparatus is briefly described. A more complete description can be found in Ref. 3 Third, some experimental results are presented. Finally, a summary and some conclusions are given.

2 PWFA CHARACTERISTICS

The linear theory for the PWFA (valid for $n_b \ll n_p$, $n_b = N/(2)^{3/2} {}_r^2 {}_z$ the e$^-$ bunch density for a bunch with N e$^-$) predicts that the largest wake amplitude a given round gaussian electron bunch with length $_z$ and radius $_r=40$ μm is [4]:

$$eE[MeV/m] = 240 \times \frac{N}{10^{10}} \left[\frac{0.6}{_z[mm]}\right]^2$$

This wake amplitude is reached in a plasma with a density such that $_p 4 _z$. However, for the typical parameter of the E-157 experiment given in Table 1, the beam/plasma interaction is in the highly non-linear regime ($n_b > n_p$, and $E_z E_{wb}= {}_p mc/e$ the cold plasma wave breaking amplitude), and 2- and 3-D Particle In Cell (PIC) numerical simulations are used to better describe the experiment. Note that these simulations essentially confirm the linear theory results. Figure 1 shows the radial (E_r) and longitudinal (E_z) wake fields excited by the beam with parameters given in Table I in a plasma with $n_p=1.5\cdot10^{14}$ cm^{-3}. The e$^-$ of the head of the bunch radially

muggli@usc.edu

expel the plasma electrons to a channel radius of r_c $2(n_b/n_p)$ $_r$. The plasma ions partially neutralize the bunch space charge, and the bunch is focused. In this experiment $n_b > n_p$ and all the plasma e$^-$ are expelled ("blow out" regime). The focusing force of the pure ion column is $F_r = -eE = -(e^2 n_p/2)r$ and has a strength of 4500 T/m in the case of Fig. 2. With this large focusing field the e$^-$ betatron wavelength $= 2 (2)^{1/2}/_p$ is shorter than the plasma, and the bunch envelope experiences multiple betatron oscillation within the plasma length. The work done by the bunch on the plasma results in a maximum decelerating field of 100 MV/m, and is experienced by the e$^-$ in the core of the bunch. The plasma e$^-$ rush back on axis and generate an accelerating gradient of several hundreds of MV/m. After 1.4 m the average energy gain by the particles in the tail of the bunch is 275 MeV. However, the maximum energy gain experienced by more than 10^8 particles (the experimental detection threshold) is of the order of 400 MeV. The average transformer ratio $E_{accel.}/E_{decel.}$ is 2.

Table 1: Typical e$^-$ beam parameters

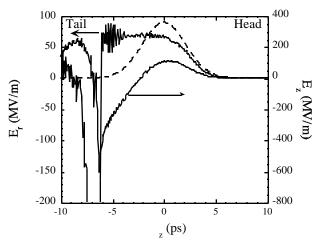|	**Symbol**	**Value**
Bunch Energy	E,	28.5 GeV, 55773
Number of e$^-$ /bunch	N	$2.0 \cdot 10^{10}$
Bunch Radius	x, y	40 μm
Bunch Length	z, z	0.7 mm, 2.3 ps
Normalized Emittance	Nx	$5 \cdot 10^{-5}$ m rad
	Ny	$0.5 \cdot 10^{-5}$ m rad

Figure 1: Transverse (E_r, thin line, left hand side scale) and longitudinal (E_z, thick line, right hand side scale) wake fields excited by the beam (shown by the doted line) with parameters given in Table 1 in a plasma with $n_p = 1.5 \cdot 10^{14}$ cm^{-3}.

3 EXPERIMENTAL SET-UP

The E-157 experimental set-up (Fig. 2) is only briefly described here, a more detailed description can be found in Ref. 3. A lithium (Li) vapor with neutral density n in the 2-4·10^{15} atoms/cm^3 is generated in a heat pipe oven [5] The Li column is about 1.4 m long and has a diameter of about 3 cm, and is confined in the oven by a He buffer gas. Lithium is chosen because of it has a low ionization potential (5.4 eV), and because it has a low atomic number (Z=3) which minimizes the beam scattering and the amount of Li impact ionization by the 28.5 GeV e$^-$ beam. An ultra-violet (uv) laser pulse at 193 nm (6.45 eV per photon) ionizes the vapor with a maximum fluence of 100 mJ/cm^2 over a 3x3 mm^2 cross section. The laser pulse is coupled into, and out of the Li column by reflection off thin SiO$_2$ coated pellicles located about 50 cm on either end of the column. The laser beam is aligned onto the spot where the e$^-$ beam traverses the pellicles, thereby aligning the plasma onto the e$^-$ beam. The uv energy incident upon, and emerging from the Li vapor is monitored by calibrated energy meters, and yield the plasma density on a single shot basis.
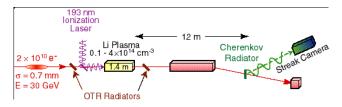

Figure 2: The E-157 experimental apparatus is shown schematically. The 28.5 GeV electrons from the SLAC linac are transported through the FFTB to IP1 (Interaction Point 1) where the plasma is located. Beam profiles are measured before and after the plasma using OTR. The FFTB permanent magnet dump, which is almost immediately after the plasma, disperses the beam at a Cherenkov radiator at IP2, 12 m from the end of the plasma. The Cherenkov light is analyzed with a streak camera to give a measurement of energy vs. time in the bunch. The plasma is a 1.4 m long Lithium vapor that is partially ionized by a 193 nm laser pulse.

The e$^-$ beam parameters (energy, emittance, position, etc.) along the FFTB line are supplied for every bunch by the SLAC Control Program. The beam size, transverse position (x-y plane), and shape before and after the plasma are obtained for each bunch by imagining the Optical Transition Radiation (OTR) light emitted by the e$^-$ when traversing thin titanium foils located 1 m on either end of the plasma (upstream and downstream). The OTR images resolution is about 20 μm. After exiting the plasma, the e beam is dispersed in energy in the vertical y plane by the dipole bending magnet of the FFTB line

dump located ~6 m from the plasma exit. The beam generates Cerenkov light in a ~1 mm thick piece of aerogel located ~12 m from the plasma exit, where the magnetic dispersion is $y=(10\ cm)\ \Delta E/E$. The Cerenkov light is split and imaged onto a CCD camera to obtain a time integrated image of each bunch. The other fraction of the light is split again, one half rotated by 90° in space and delayed in time. Both halves are sent to a streak camera to obtain the time resolved image of the bunch spot size in the x plane ($\sigma_x(t)$, in the plane without dispersion), and the time resolved bunch energy spectrum in the y plane ($E(t)$, in the plane with dispersion). The spatial resolution of these images is ~100 μm, corresponding to an energy resolution of ~30 MeV in the y plane. The time resolution for both images is ~1 ps. The synchrotron radiation emitted by the beam along its betatron trajectory is monitored at the end of the FFTB gamma ray line.

4 EXPERIMENTAL RESULTS

4.1 Betatron Oscillations

Figure 3 shows the spot size (σ_x) of the e beam in the x plane measured at the downstream OTR location, as a function of the relative uv laser pulse energy. The plasma density is proportional to the uv pulse energy. The values of σ_x are obtained from gaussian fit to the projected OTR images. The first minimum (low uv energy) of σ_x on Fig. 3 corresponds to the plasma lensing action of the plasma on the beam. The subsequent minima correspond to the multiple betatron oscillations of the beam envelope within the plasma length [6]. Assuming the beam transport parameters α, β, γ of the beam at the plasma entrance are known, the line integrated plasma density ($\int n_p^{1/2}(z)dz=n_p^{1/2}L$ for a constant n_p over L) as a function of the relative uv energy can be deduced. In particular, the plasma length $L=1.4$ m was chosen such that the 4th minimum of Fig. 3 corresponds to the optimum n_p for a beam with $\sigma_z=07$ mm ($\beta_p\approx4\sigma_z$): $n_p\approx1.5\cdot10^{14}$ cm^{-3}. At this value of n_p, the beam size in the Cerenkov energy diagnostic plane is also minimum, which leads the best energy resolution (≈30 eV). Evidence of dynamic focusing within one single bunch was observed with large (≈100 μm) beams.

4.2 Tail Flipping

Transverse fields in the linac generate beam tails, i.e., trailing e⁻ which are not distributed around the beam axis, as defined by the bunch head trajectory. The transverse field of the plasma wake imparts a transverse momentum to the tail with an amplitude at the plasma exit that varies with n_p. Figure 4 shows the bunch centroid oscillation resulting from the bunch tail "flipping" by the plasma, as measured by a beam position monitor located ~2.5 m downstream from the plasma exit. This data was acquired at the same time as the beam spot size data shown on

Fig. 3. Note that, as expected, the tail flipping is correlated with the bunch spot size oscillation (Fig. 3) [7].
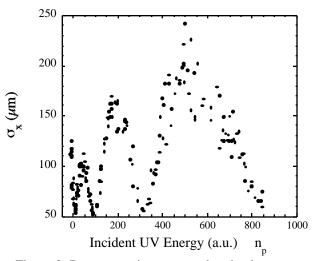

Figure 3: Beam spot size measured at the downstream OTR location as a function of the relative uv laser pulse energy. The plasma density is proportional to the uv energy.
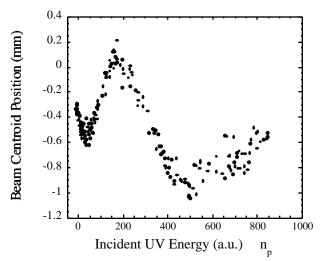

Figure 4: Beam centroid position measured by a beam position monitor located ~2.5 m downstream from the plasma exit. This data was acquired at the same time as the beam spot size data shown on Fig. 3.

4.3 Hose Instability

An e⁻ bunch propagating in a long plasma is subject to the hose instability [8]. This instability can disrupt the e⁻ bunch, and severely limit the amount of energy the e⁻ can gain in the PWFA. Studying the motion of the bunch tail, used as a seed or probe for the hose instability, shows that no instability is observed over the parameter range of the E-157 experiment. A similar conclusion is obtained from 3-D PIC simulations with the E-157 parameters [9]. These results disagree with the linear

theory for the instability in the short bunch limit, which predicts a growth by a factor of 3 over the 1.5 m plasma [8].

4.4 Synchrotron Radiation

The e⁻ emit synchrotron radiation in the x-ray range along their betatron trajectory. The plasma acts on the e⁻ as a very simple wiggler and could be used to produce radiation in the visible to x-ray range (Ion Channel Laser [10]). The spontaneous radiation is detected using surface barrier detectors located at the end of the FFTB gamma ray line. The x-ray photons are Bragg refracted according to their energy by a thin Si wafer in the (111) crystalline orientation. The amplitude of the incoherent scattered signal varies with the square of the plasma density, and is proportional to the total radiated power [11].

4.5 Beam Steering

The photo-ionized plasma is long and has a small transverse cross-section (3x3 mm²). The angle between the ionizing laser pulse (i.e., the plasma) and the electron beam can be varied. When the e⁻ beam crosses the transverse boundary between the plasma and the neutral Li vapor is experiences a deviation of its trajectory [12] similar to that experienced by a ray of light at a dielectric boundary (refraction a water/air interface for example). The angle of deviation follows a non-linear Snell's law. This phenomenon has been discovered and observed for the first time in this experiment.

4.6 Energy Loss and Gain

Time resolved energy spectra are obtained from streak camera images of the beam in the energy dispersive plane after the FFTB dipole dump magnet. For the analysis [13] the beam image is cut in time slices of 1 ps (the streak camera temporal resolution) and the mean energy of each slice is calculated. A sample of this analysis for several events is shown in Figure 5. In this example, the core of the beam lost an average of 30 MeV while the electrons in the last tail slice gained an average of 120 MeV.

A typical streak camera image obtained at the optimum plasma density is displayed in Figure 6. This image shows the same energy loss and gain in the beam slice centroids (Fig. 6), and also shows particles, appearing as single events on the image, accelerated to even higher energies. Notice the qualitative difference between the two streaks. Without an imaging magnetic spectrometer these results are sensitive to the behavior of the bunch tail and to the energy dependent focusing properties of the plasma on the beam (chromaticity). Thus, a good understanding of beam transverse dynamics in the plasma is necessary for a complete understanding of the beam longitudinal dynamics.
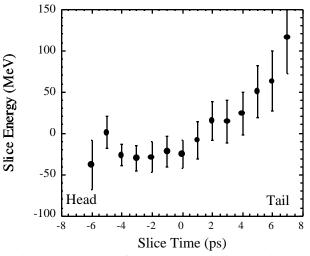

Figure 5: Result of the slice analysis showing the average energy of 1 ps slices obtained from 23 individual images. The core (-2 ps) of the beam looses energy, where as the slices in the tail gain energy (see Fig. 2).
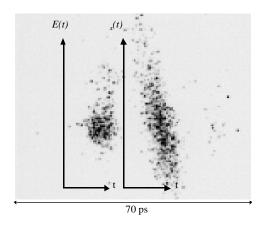

Figure 6: Streak camera image showing the beam energy as a function of time ($E(t)$) on the left hand side, and the beam spot size in the x plane as a function of time ($_x(t)$) on the left hand side. Notice the qualitative difference between the 2 streaks. This image was used in the slice analysis shown on Fig. 5.

5 SUMMARY AND CONCLUSIONS

The E-157 experiment is the first attempt to study the issues related to a meter long plasma accelerator module relevant for high-energy colliders. A 1.4 meter long plasma source with a density in the 10^{14} cm⁻³ range has been developed. The transverse dynamics of the e⁻ beam propagating in the meter long plasma has been studied (plasma focusing, betatron oscillations, tail flipping, and hose instability). The emission of x-ray radiation by the e⁻ in the plasma ion channel has been observed. New physics has been discovered: the bending of the 28.5 GeV e⁻ beam by the tenuous plasma at the plasma/vapor interface. The measurement of the energy gain by the

bunch trailing e⁻ is more difficult than anticipated, and depends critically on the understanding of the transverse beam dynamics in the PWFA. However, the matching of the beam to the plasma channel, and the use of an imaging magnetic spectrometer should greatly reduce the influence of the beams transverse dynamics in future experiments. The same experiments should be performed with a positron beam to demonstrate the relevance of the PWFA to future high-energy colliders.

ACKNOWLEDGEMENT

REFERENCES

[1] D. Gordon *et al.*, Phys. Rev. Lett. 80(10) 2133 (1998).

[2] R. Assmann *et al*., Nucl. Inst. Meth. Phys. Res. A 410 396 (1998).

[3] M. Hogan *et al.*, Phys. of Plasmas 7 2241 (2000).

[4] S. Lee *et al.*, Phys. Rev. E 61 7014 (2000).

[5] C.R. Vidal and J. Cooper, J. Appl. Phys. 40(8) 3370 (1960), P. Muggli *et al.*, IEEE Trans. Plasma Sci. 27(3) 791 (1999).

[6] C.E. Clayton *et al.*, to be submitted to Phys. Rev. Lett..

[7] B.E. Blue *et al.*, to be submitted to Phys. Rev. Lett.

[8] D.H. Whittum *et al.* Phys. Rev. Lett. 67 991 (1991), A. Geraci and D. H. Whittum, Phys. Plasmas 7 3431 (2000).

[9] E.S. Dodd *et al.*, to be submitted to Phys. Rev. Lett.

[10] D.H. Whittum *et al.,* Phys. Rev. Lett. 64 2511 (1990).

[11] S. Wang *et al.*, to be submitted to Phys. Rev. Lett.

[12] P. Muggli *et al.*, submitted to Nature, October (2000).

[13] M. Hogan *et al.*, to be submitted to Science.